



Published in final edited form as:

Arthritis Rheum. 2009 June ; 60(6): 1694–1703. doi:10.1002/art.24520.

A ROLE FOR GAMMA DELTA T-CELLS IN A MOUSE MODEL OF FRACTURE HEALING

Nona T. Colburn, M.D.¹, Kristien J.M. Zaal, Ph.D.², Frances Wang, Ph.D.³, James Yen, Ph.D.³, and Rocky S. Tuan, Ph.D.¹

¹Cartilage Biology and Orthopaedic Branch, National Institute of Arthritis and Musculoskeletal and Skin Disease, National Institutes of Health, Department of Health and Human Services, Bethesda, Maryland 20892

²Light Imaging Section, National Institute of Arthritis and Musculoskeletal and Skin Disease, National Institutes of Health, Department of Health and Human Services, Bethesda, Maryland 20892

³Polymers Division, National Institutes of Standards and Technologies, Gaithersburg, Maryland 20899

Abstract

Objective—Fractures can initiate an immune response that disturbs osteoblastic and osteoclastic cellular homeostasis through cytokine production and release. The aim of our study was to investigate $\gamma\delta$ T-cells, innate lymphocytes known to be involved in tissue repair, as potential cellular components of the osteoimmune's system response to an in-vivo model of bony injury. The absence of such cells or their effector cytokines influences the fate of other responder cells in proliferation, differentiation, matrix production, and ultimate callus formation.

Methods—Tibia fractures were created in 60 $\gamma\delta$ T-cell receptor knockout and 60 control C57BL/6 mice. Analysis included radiographs, basic histology, mechanical testing, flow cytometry, and immunohistochemical localization of $\gamma\delta$ positive subsets from control animals, and of CD 44 from both groups, as well as ELISA for the effector cytokines, IL-2, interferon- γ , and IL-6, respectively.

Results— $\gamma\delta$ knockout animals demonstrated more mature histological elements and quantitative increases in the expression of major bone (bone sialoprotein) and cartilage (collagen type II) matrix proteins, and bone morphogenetic protein-2 at a critical reparative phase. Moreover, only knockout animals had a decrease in osteoprogenitor antiproliferative cytokines, IL-6 and interferon- γ . The result was improved stability at the repair site and an overall superior biomechanical strength in knockout mice as compared with controls.

Conclusion—The evidence for $\gamma\delta$ T-cells in the context of skeletal injury demonstrates the importance of the immune system's impact on bone biology, relevant to the field of osteoimmunology, and offers a potential molecular platform from which to develop essential therapeutic strategies.

Keywords

osteoimmunology; $\gamma\delta$ T-cells; fracture healing; biomechanical testing; $\gamma\delta$ -deficient mice; cytokines; innate immunity

Introduction

Bone injuries present an important health concern, as they can result in disfigurement, pain, loss of mobility and productivity, and post-traumatic osteoarthritis. (1) Although there are many well recognized factors and systemic states associated with bone healing abnormalities,(2) the molecular cascade of events or the specific aberration that occurs when normal bone repair fails is not well understood. Previous research efforts on optimizing fracture repair have been directed primarily at different pathways of the cellular response involved in induction of osteoprogenitor cells into bone forming cells, especially using growth factors, such as fibroblast growth factors (FGFs) and bone morphogenetic proteins (BMPs).(3,4)

The first and immediate response to endogenous signals of cell and tissue injury(5) is an inflammatory reaction frequently modeled in the skin,(6) as well as the systemic host response.(7) Fracture injury initiates an osteoimmunological response through multiple interrelated pathways that ultimately disturbs osteoblastic and osteoclastic cellular homeostasis.(8) Cytokines, growth factors, and BMPs present in this milieu act as signal transducers that effect subsequent stages of repair through progenitor cell recruitment, proliferation, and matrix synthesis.(9,10) While most are mitogenic, some cytokines, such as IL-6 and interferon- γ , can decrease bone formation by influencing bone resorption(11) and exhibiting antiproliferative effects, especially on the osteoblast.(12) Finite element models have demonstrated the capacity for early cell fate decision within the first 5 days.(13) Therefore, for the progression of the four phases of bone regeneration(14) and the final bone product (15), it is critical that the initial inflammatory stage be specific and controlled. Non-steroidal anti-inflammatory drugs,(16,17) antihistamines,(18) steroids,(19) and cyclooxygenase-2 (COX-2) inhibitors,(17) which inhibit the inflammatory response, can delay fracture healing.

In normal human fracture injury, $\alpha\beta$ T-lymphocytes are selectively recruited and activated. They are consistently present in the early inflammatory phase(20) at which time they are the major producers of IL-2, and act as potent stimulators of mesodermal cell division(3,9) and osteoinduction.(21). Direct evidence for T-cell involvement in the control of fracture healing is provided by both in-vitro(21,22) and in-vivo(20,23–25) studies, which have demonstrated negative effects of lymphocyte depletion on fracture healing outcome. Multiple signaling pathways interrelate T-cell immunity with skeletal regeneration. Receptor activator for nuclear factor κ B ligand (RANKL) expressed by osteoclast is a key regulator of bone resorption in fracture healing.(26) Intriguingly, RANKL also regulates T-cell dendritic cell communications and T-cell activation.(27)

$\gamma\delta$ T-cells, as “innate lymphocytes”, have the unique ability to directly recognize products of stressed cells through their receptor without the need for antigen presenting cells. They produce cytokines that are predominately Th1 (interferon- γ).(28) However, depending on the context, $\gamma\delta$ T-cells can also make Th-2 cytokines, as well as IL-17 through induction of Th17 cells by ROR γ t+ cells.(29) The type of cytokine produced is determined not only by differences in the disease models, but also by the cytolytic ability of $\gamma\delta$ T-cells that express FasL. (30) In addition, $\gamma\delta$ T-cells may assist in dictating the Th1 or Th2 phenotype of the CD4+ $\alpha\beta$ T-cell response.(31,32)

Although the exact biological function of $\gamma\delta$ T-cells remains unanswered, genetically engineered deficient experimental models have focused on an immunoregulatory role. (33–35) They can perform specialized functions related to the repair of tissue damage (28,36,37) and wound healing.(38) The molecular basis of tissue localization at sites of injury by $\gamma\delta$ T-cells is currently unknown. One receptor that facilitates their migration and extravasation to

areas of inflammation is CD44.(39) The CD44 receptor, up-regulated by both lymphocytes (39) and bone cells (40) binds hyaluronan in association with wound and bone regeneration. In a $\gamma\delta$ T-cell receptor (TCR) knockout mouse model, $\gamma\delta$ T-cells are required for hyaluronan deposition, subsequent macrophage infiltration into wound sites, and appropriate wound repair.(41)

The aim of our study was first, to demonstrate that $\gamma\delta$ T-cells, as part of an innate immunological response to injury, would be recruited to the local site of fracture repair. Secondly, we investigated the consequence of the absence of $\gamma\delta$ T-cells to the final outcome of the repair product. We hypothesized that the absence of $\gamma\delta$ T-cells would impact negatively on cellular proliferation, adhesion, differentiation and ultimate callus formation, not unlike that already seen with wound healing.

Material and Methods

The study was carried out with approval of the NIH Animal Care and Use Committee.

Animal model

Mice homozygous for the $Tcrd^{tm1mom}$ delta chain targeted mutation and C57BL/6 background wild type controls were from Jackson Laboratories (Bar Harbor, ME). A 4 kb deletion encompassing most of the delta chain constant region sequences, results in $\gamma\delta$ T-cell receptor deficiency in all adult lymphoid and epithelial organs, in the presence of normal development of the $\gamma\delta$ T-cell lineage. Additionally, this mutation does not impact the number or function of B-cells, the expression of several cell surface markers including LFA-1, CD-2, CD69, and IL-2, or T-helper function in animals aged 4 weeks. (42)

Sixty adult male $\gamma\delta$ knockout mice and sixty control mice (23–28 g) aged 6 weeks were assigned to six groups: (1) histology (8 controls, 10 knockouts); (2) immunohistochemistry (4 controls, 5 knockouts); (3) semiquantitative reverse transcription-polymerase chain reaction (RT-PCR) 8 in both groups); (4) ELISA (8 in both groups); (5) flow cytometry (9 pre-operative animals in each group, 14 control and 12 knockout animals); and (6) mechanical testing and tissue geometry analysis (9 controls and 8 knockouts).

Fracture procedure

Under general isoflurane anesthesia, fractures were created in the right mid tibia by three-point bending using a custom-built fracture apparatus and then instrumented with intramedullary pins. Fracture healing (four phases) was evaluated at 1, 5, 10, and 28 days in groups 1– 5. For biomechanical testing and histomorphometry, tissues were processed at 2, 4, 6, and 8 weeks. Radiographic analysis at each time point was scored as 0, 1, or 2 based on quality of union with the presence, partial presence, or absence of the fracture line, respectively.

Histology

Calluses were excised, fixed in phosphate-buffered 4% paraformaldehyde (pH 7.2) for 3 days at room temperature, and decalcified in 20% ethylenediaminetetraacetic acid at room temperature for 7 days. The tissue samples were then dehydrated through a graded ethanol series and paraffin embedded. Sections of 10 μ m thickness were obtained through the entire callus, and stained with Masson-Trichrome, hematoxylin and eosin. Blind histological scoring was done according to Bos *et al*, (43) with modification. Scores of 0 through 5 were assigned to two categories for quality of union and colonization of bone marrow, based on callus maturity and bone marrow reconstitution, respectively.

Immunohistochemistry (IHC)

Calluses were excised, fixed, decalcified, and paraffin embedded as above. Three serial sections from both knockout and controls at each time point were used for CD 44 immunostaining. Controls alone were immunostained for $\gamma\delta$ TCR. The avidin-biotin-peroxidase complex method of Hsu *et al* (44) was used with a kit. (Zymed, San Francisco, CA). Sections were deparaffinized, rehydrated, and treated with 3% hydrogen peroxide in 100% methanol for 20 minutes to block endogenous peroxidase activity. Horseradish peroxidase (HRP) activity was detected using hydrogen peroxide as substrate and chromagen aminoethylcarbazole (AEC) as dye, and hematoxylin as counterstain. Negative controls were incubated with non-immune isotype antibodies (Figure S-1). Sequential changes in CD44 and $\gamma\delta$ TCR immunoreactivities regarding percentage and types of cells stained at four phases of fracture healing were scored according to Fujii *et al.* (45).

Real-time polymerase chain reaction (RT-PCR)

Messenger RNA expression of bone sialoprotein (BSP), collagen type II, and BMP-2 was analyzed to assess the progression of fracture repair. Calluses were harvested with 3 mm of bone proximal and distal to the fracture site, snap-frozen in liquid nitrogen and stored at -80°C . Two specimens each from control and knockout were pooled for each time point and total RNA was isolated using Trizol. Semi-quantitative PCR was performed for 30 cycles on single-strand complementary DNA (cDNA) prepared from RNA (1 μg) using a SuperScript One-Step RT-PCR with Platinum *Taq* (Invitrogen Life Technologies Carlsbad, CA). The gene specific primer sequences (46–48) (IDT Coralville, IA) and the expected PCR product sizes are listed in Table S-1. Amplification was as follows: denaturation: 94° , 30 seconds; annealing: 53° , 45 seconds; extension: 72° , 60 seconds. GAPDH was used as control for integrity of various RNA preparations and RNA load. The PCR products were gel separated and images analyzed by densitometry.

Enzyme-linked immunosorbent assay (ELISA)

Calluses were harvested and homogenized as above. Two specimens each from control and knockout were pooled per time point. Homogenates were centrifuged (15,000 rpm, 15 minutes, 4°) for debris removal. Supernatants were analyzed for cytokines, INF- γ , IL-2, and IL-6, with commercially ELISA kits (Quantikine M; R & D Systems, Minneapolis, MN). Assays were done in triplicate. The plates were read at 405 nm. All data were normalized to total protein concentrations. Cytokine concentrations (pg/ml) were presented as mean \pm standard error.

Flow cytometry

In order to analyze the systemic response distant from the site of injury, flow cytometry analysis of total lymphocyte counts, subset $\gamma\delta$ T-cells, and cells expressing the CD44 marker were performed on peripheral blood. Lymphocytes were fractionated using Ficoll gradient centrifugation. Cell suspensions containing 1×10^5 cells were incubated for 30 minutes at room temperature with either conjugated anti-CD44-phycoerythrin (PE) or anti- $\gamma\delta$ TCR-Tricolor (1:100 in PBS with 1% bovine serum albumin and 0.1% sodium azide). Cells were washed and fixed in 1% paraformaldehyde. Non-specific mouse IgG was used as negative control. Results were reported as percent of cells positive for each fluorochrome with gating at the 98th percentile of isotype stained cells. Data from up to 100,000 cells were acquired and analyzed using appropriate compensation with both CellQuest (BD Beckman) and FlowJo (Treestar) software.

Mechanical testing and tissue geometry

Bilateral fractured and unfractured tibias were harvested and tested fresh, with the intramedullary pin extracted. The maximum vertical (D_v) and horizontal (D_h) diameter of the gross callus, and the mid-diaphysis of the unfractured tibia were measured prior to mechanical testing. Transverse diameters of the marrow space were measured from anteroposterior radiographs using the nail diameter as reference. This allowed geometric calculations of callus quantity, expressed as callus area (X_a), and the area moment of inertia (I) for the load direction, assuming elliptical cross sections with centrally located holes. These formulae were used:(49)

$$X_a (\text{mm}^2/\text{g}) = \pi(D_v/2)(D_h/2) \quad (\text{The average callus area was adjusted for the weight (gram) of each animal.}) \quad (1)$$

$$I (\text{mm}^4) = (\pi/64)D_h D_v^3 \quad (2)$$

Biomechanical properties of healing fractures were analyzed by a destructive three-point bending procedure on a materials testing machine (Instron Model). The callus was positioned on two grooved roller supports of a holding apparatus, spanning a total distance of 6.5 mm with the repair site centered. The machine settings were: maximum local value, 50 N; chart speed, 10 sec/cm; crosshead speed, 2 mm/minute. A load displacement curve was produced as loading was continued until the specimens exhibited failure (F). (Figure S-2) From this curve the following structural or extrinsic parameters were obtained: maximum load (P_{\max}) (N), deflection at maximum load (D_{\max})(mm) and maximum stiffness (N/mm), defined as the slope ($K = \Delta P/\Delta D$). With the slope (K) and the test span ($L=6.5$ mm) the rigidity (R) was calculated as follows:(50)

$$R (\text{N/mm}^2) = (K)L^3/48 \quad (3)$$

In addition to structural parameters, the intrinsic or material properties, elastic modulus (E) and stress (σ), were calculated using standard engineering formula derived from simple beam theory. (50) Both material properties, as a function of applied load and moment of inertia, are dictated by callus geometry and therefore reflect properties at the periosteal surface.

$$E (\text{N/mm}^2) = (L^3)(K)/48(I) \quad (4)$$

$$\sigma (\text{N/mm}^2) = (ML)(L)(C)/4(I) \quad \text{where } C \text{ is } \frac{1}{2} D_h \quad (5)$$

Another material property calculated was the ability of the healing bone to absorb energy during loading. This is the area under the curve, either to maximum load or failure, and is a function of both load and deflection. (Figure S-2)

Statistics

Data are reported as mean and standard deviation (error bars: \pm SD). Data points were distributed around the mean in a normal fashion and did not require transformation. Two

samples were compared using Student's t-test. Statistical analysis of mechanical testing data was examined for normal distribution and homogeneity of variances (F-test) using the GLM procedure of SAS. Differences were judged as statistically significant at $p \leq 0.05$.

Results

$\gamma\delta$ T-cells respond to fracture injury

To better assess the relevance of the $\gamma\delta$ knockout mice as an experimental model, the actual presence of $\gamma\delta$ T-cells at the local fracture repair site was first identified in control animals by immunohistochemistry of $\gamma\delta$ TCR. Representative micrographs for the four phases of fracture healing (days 1, 5, 10, and 28) are shown in Figure 1. At the time of fracture, the $\gamma\delta$ T-cells were localized within the hematoma (Figure 1A). In the ensuing inflammatory phase, when the hematoma was replaced with an accumulation of monocytes, macrophages, and immature mesenchymal cells, $\gamma\delta$ TCR staining was found distributed on both inflammatory and mesenchymal cells. At Day 5, as the fracture callus began to form, more $\gamma\delta$ TCR positive cells are found with the morphological appearance of fibroblastic mesenchymal cells (Figure 1B). During both the chondrogenic and osteogenic phases, $\gamma\delta$ TCR staining was detected on osteoblasts lining trabecular bone (Figure 1C). On Day 28, as the bony callus is remodeled, $\gamma\delta$ TCR staining was not observed, being specifically absent within lacunae (osteocytes) (Figure 1D), as well as the maturing cartilage at all time points. Table 1 shows a summary of the immunohistochemical analyses for $\gamma\delta$ TCR staining in control animals, as well as CD44 staining for both control and knockout mice, at different phases of fracture repair.

In trauma patients, $\gamma\delta$ T-cells decrease immediately in the peripheral blood after injury with increased homing into local lymphoid tissue until the third day.(51) When $\gamma\delta$ T-cells responded to the local fracture site in control animals, their presence was also noted peripherally by flow cytometry. (data not shown) The percentage of cells expressing the $\gamma\delta$ TCR receptors decreased immediately after injury, but increased significantly ($p < 0.05$) above baseline at Day 10. This peak level of peripheral $\gamma\delta$ TCR positive cells occurred at the same time as the maximal level of immunohistochemical staining at the fracture site.

$\gamma\delta$ Knockout animals demonstrate early differences in cartilage and bone formation

Although typical histological features were seen in a sequential fashion in both groups, $\gamma\delta$ knockout animals exhibited better quality of union with more osseous and chondral elements and mature bone marrow at Day 5 (Figure 2A and B). This improvement was supported at a molecular level by increased mRNA expression of cartilage and bone associated markers, including collagen type II, BSP, and BMP-2 (Figure 2C). However, these differences were not observed as the callus matured. Consistent with previous studies,(52) mRNA expression of these three genes were observed during all phases of fracture healing and correlated with the histological appearance. With radiographic evaluation it was noted that knockout animals did not demonstrate improved healing over controls until Day 28. (data not shown)

$\gamma\delta$ Knockout animals produce less inflammatory cytokines at the regenerative site

With the absence of $\gamma\delta$ T-cells, $\gamma\delta$ knockout animals showed a significant decrease ($p < 0.05$) in the production of IL-2 at the inflammatory phase (Day 1) and interferon- γ and IL-6 at the reparative phase (Days 5 and 10) in fractured bones as noted by ELISA (Figure 3 A, B, and C). In previous studies of cytokine production by fracture calluses as shown by relative message, IL-6 demonstrated high constitutive activity early at day 3 in normal animals.(11)

$\gamma\delta$ Knockout animals up-regulate the cell adhesion molecule, CD44 in osteoblasts

At the local fracture site, as shown by IHC in Table 1, several cell types throughout the healing process expressed CD44, consistent with previous studies.(40) However, important spatial and temporal differences in CD44 expression were noted between $\gamma\delta$ knockouts and controls. Early on days 1 and 5, only $\gamma\delta$ knockout animals demonstrated CD44 expression within the hematoma and on osteocytes, respectively. Moreover, during the reparative phases, only $\gamma\delta$ knockout animals showed positive staining for CD44 cell adhesion molecule in osteoblasts, not seen in previous reports (Figure 4A).

For assessment of lymphocyte homing, cells gated for total lymphocytes in both $\gamma\delta$ knockout and controls (figure 4B) and $\gamma\delta$ TCR positive lymphocytes in controls alone (figure 4C) were analyzed for CD44 expression by flow cytometry. A significant decrease in CD44 expressing peripheral lymphocytes was noted on Day 5 in knockout animals compared to controls. However, by Days 10 and 28, this difference was lost. Taken together, these results showed that temporal profiles of both the $\gamma\delta$ TCR and CD44 surface markers followed that of total $\gamma\delta$ T-cells, but with a decreased percentage of positive cells from day 1 through day 28. It is likely that these decreases were consequences of stress induced alterations in normal cell trafficking, resulting in depletion of circulating lymphocytes expressing surface CD44 adhesion molecules, perhaps via a homing mechanism that redistributed cells from blood to sequestration at sites of inflammation.(51, 53, 54)

Biomechanical properties of fracture repair are superior in the absence of $\gamma\delta$ T-cells

Both structural (rigidity) and material (elastic modulus) strength variables were different between $\gamma\delta$ knockout and control mice (Figure 5A). The average maximum rigidity of the healing fractures in $\gamma\delta$ knockout mice were 241, 57, and 17% of the maximum rigidity sustained by controls at 4, 6, and 8 weeks, respectively, while elastic modulus were 785, 55, and 82%, respectively, compared with the corresponding values for controls. At all five points, $\gamma\delta$ knockout animals reached statistically significant higher values of maximum load ($p=0.0002$), stiffness ($p=0.05$), and elastic modulus ($p=0.05$) before failure compared with controls. The $\gamma\delta$ knockout animals had comparatively higher values of maximum stress than controls, but were not statistically significant ($p=0.09$). At 8 weeks, $\gamma\delta$ knockout animals showed essentially no significant differences compared to controls with respect to maximum load ($p=0.27$), rigidity ($p=0.46$), and elastic modulus ($p=0.45$).

This overall increase in strength was also reflected in the larger amount of energy to failure when $\gamma\delta$ knockout animals were compared with controls ($p=0.03$). (Figure 5B) In the 4-week knockout group, energy absorbed to failure was 47% greater than that of controls. However, at 6 and 8 weeks the gap narrowed to 10 and 6 % respectively, so that at 8 weeks there was no statistically significant difference between the ability of $\gamma\delta$ knockout callus to absorb energy than that of control callus ($p=0.76$) Tibia fractures in mice are usually considered healed when strength has reached values of contralateral intact bone, thus acting as an internal control. At 4 weeks, the fractured tibias of $\gamma\delta$ knockout animals had reached 85 and 42% of the rigidity and elastic modulus of the corresponding values of intact bones, whereas the rigidity and elastic modulus of control animals had only reached 28 and 6% of intact bone. Structurally, with respect to stiffness and rigidity, $\gamma\delta$ knockout callus more closely approximated values of intact bone for all weeks ($p=0.07$), than controls that demonstrated statistically greater differences between fractured and intact bone. ($p<0.0001$) Data obtained for both the healing right tibia and the contralateral intact bone are available as supplementary tables (Tables S-2, 3, and 4).

Discussion

This work demonstrates, for the first time, the expression of $\gamma\delta$ T-cells in response to fracture injury, as well as the concept that $\gamma\delta$ cells and/or their attendant cytokines could play a detrimental role in bone healing. When $\gamma\delta$ T-cells are not present, overall improved biomechanical strength and stability, as a final outcome, is seen in knockout animals compared to that of controls. Histological, immunohistochemical and molecular analyses corroborate these findings with quantitative increases in osseous and chondral elements, temporal augmentation in the gene expression of collagen type II, BSP, and BMP-2, and increased CD44 expression in matrix producing osteoblasts, providing a potential explanation for the significant biomechanical stability noted.

These observations support the view that $\gamma\delta$ T-cells, as a part of the innate immune system's response to "danger signals", play a part in the surveillance of body surfaces that are exposed to environmental hazards.(28) In principle, the initial inflammatory phase of fracture injury, acting as an immunological response, would activate $\gamma\delta$ T-cells that respond with the production of proinflammatory and Th-1 effector cytokines, such as interferon- γ and IL-6. During the first days after fracture, the cytokines and growth factors released are important determinants of future phases of bone regeneration. Once the initial inflammatory phase has passed, and apoptosis of cells no longer induces danger signals, the immune response stops, and maturation of the callus would proceed. It is likely that the $\gamma\delta$ cell population responding to fracture injury represents a distinct sublineage, differing not only in their TCR, but also in homing receptors and other properties.

The action of $\gamma\delta$ cells in fracture healing is likely mediated through changes in biological activities of resident cartilage and bone cell populations influenced by a decrease in inflammatory cytokine production at the regenerative site. Precisely how other cells interpret the changed immunological milieu when $\gamma\delta$ cells are absent and the subsequent effect on the local osteoinductive sequence with chondrocyte and osteoblast differentiation is open to speculation. In this context, Th1 cytokines such as interferon- γ and IL-6 released within the microenvironment in which $\gamma\delta$ cells reside could, under appropriate systemic conditions, play an antagonistic role to osteoprogenitor cells responsible later for bone repair.

In this study, within 5 days, the absence of $\gamma\delta$ T-cells has exhibited a qualitative influence on the final regenerative product. Both initial molecular signals, that influence the commitment and differentiation of mesenchymal cells to an osteogenic or chondrogenic lineage, as well as signals that regulate cell proliferation and terminal differentiation during later stages are likely to be involved.(13). In the face of a dynamic challenge, early changes noted in bone and cartilage formation in the $\gamma\delta$ knockout animal may reflect the impact of the reorganization of the immunological milieu at the inflammatory stage. Eventually as later pathways become involved differences are narrowed or lost.

Different outcomes for fracture healing at different time points may possibly reflect the dual and diverse roles that have been recognized for subsets of $\gamma\delta$ T-cells. For example, when $V\gamma 1+$ and $V\gamma 4+$ were depleted in a collagen induced arthritis model, the $V\gamma 4+$ subset expressed high levels of CD44 within the first nine days of the disease.(55) In addition, the intense lytic activity of the $\gamma\delta$ T-cell can influence the early cytokine environment in a Fas-dependent manner and may determine which population of responding cells are targeted for apoptosis.(30) Such characteristics of $\gamma\delta$ T-cells could play major roles in how the inflammatory stage is resolved in fracture healing.

In terms of tissue geometry, the $\gamma\delta$ knockout callus was found to be of a smaller and more compact size when compared to controls. This would correlate with a decrease in cartilage formation, an increase in ossified matrix, and a stimulation of osteoblastic activity, perhaps

cell adhesion, all of which reflect a decrease in periosteal and endosteal expansion. The increased strength noted in a callus of smaller size is best explained in a three-fold manner. First, since T-cells may represent a population of osteoinductive cells,(21) their number is understandably reduced in $\gamma\delta$ knockout animals, and subsequently less cells would be induced to respond initially, creating a smaller template. Second, the environmental milieu that pervades in the absence of $\gamma\delta$ T-cells may permit an increased proliferative capacity for those undifferentiated cells that remain at the injury site, perhaps through the down regulation of interferon- γ and IL-6. This switch in cytokine profile may up-regulate an $\alpha\beta$ T-cell response that is more conducive to cell proliferation and differentiation.(32) Third, the expression of CD44 in matrix producing osteoblast of $\gamma\delta$ knockout animals may confer stability during the early reparative phase. Previously, CD44 has been recognized as an osteoclast and osteocyte surface receptor primarily seen during the later remodeling phase of fracture.(40)

In this dynamic model of fracture injury, future study will be necessary in order to establish the biological relevance of a $\gamma\delta$ T-cell response at the fracture site. Distinct properties that are lineage and receptor specific, such as subset identification, adhesion marker and cytokine profiling should be characterized for the $\gamma\delta$ T-cell, as well as the impact of their loss on $\alpha\beta$ T-lymphocytes, B-cells, and other immune modulators. Manipulations that target restoration of cellular homeostasis through modulation of cytokine production and specific interactions that exist between the immune and musculoskeletal systems as a result of skeletal injury could lead to an effective approach for decreasing the frequency of nonunion in susceptible patients. Although early systemic therapy with immunosuppressants directed at proinflammatory cytokines might be considered, therapies directed at discreet small molecules of the $\gamma\delta$ pathway could prove more tissue specific and decrease attendant side effects. Genetic and molecular regulation of the influence of $\gamma\delta$ T-cells during the initial phase of fracture healing should be explored from an immunological prospective.

Supplementary Material

Refer to Web version on PubMed Central for supplementary material.

Acknowledgments

This research was supported by the Intramural Research Program of NIAMS, NIH (Z01 AR-41131) and the National Institute of Standards and Technologies.

References

1. Einhorn TA. Enhancement of fracture-healing. *J Bone Joint Surg Am.* 1995; 77(6):940–956. [PubMed: 7782368]
2. Hayda RA, Brighton CT, Esterhai JL Jr. Pathophysiology of delayed healing. *Clin Orthop Relat Res.* 1998; (355 Suppl):S31–S40. [PubMed: 9917624]
3. Bolander ME. Regulation of fracture repair by growth factors. *Proc Soc Exp Biol Med.* 1992; 200(2):165–170. [PubMed: 1374563]
4. Trippel SB. Growth factors as therapeutic agents. *Instr Course Lect.* 1997; 46:473–476. [PubMed: 9143989]
5. Matzinger P. An innate sense of danger. *Semin Immunol.* 1998; 10(5):399–415. [PubMed: 9840976]
6. Barbul A, Regan MC. The regulatory role of T lymphocytes in wound healing. *J Trauma.* 1990; 30(12 Suppl):S97–S100. [PubMed: 2254999]
7. Miller SE, Miller CL, Trunkey DD. The immune consequences of trauma. *Surg Clin North Am.* 1982; 62(1):167–181. [PubMed: 7199763]

8. Wichmann MW, Arnoczky SP, DeMaso CM, Ayala A, Chaudry IH. Depressed osteoblast activity and increased osteocyte necrosis after closed bone fracture and hemorrhagic shock. *J Trauma*. 1996; 41(4):628–633. [PubMed: 8858020]
9. Canalis E. Effect of growth factors on bone cell replication and differentiation. *Clin Orthop Relat Res*. 1985; (193):246–263. [PubMed: 3882294]
10. Frost HM. The biology of fracture healing. An overview for clinicians. Part I. *Clin Orthop Relat Res*. 1989; (248):283–293. [PubMed: 2680202]
11. Einhorn TA, Majeska RJ, Rush EB, Levine PM, Horowitz MC. The expression of cytokine activity by fracture callus. *J Bone Miner Res*. 1995; 10(8):1272–1281. [PubMed: 8585432]
12. Gowen M, MacDonald BR, Russell RG. Actions of recombinant human gamma-interferon and tumor necrosis factor alpha on the proliferation and osteoblastic characteristics of human trabecular bone cells in vitro. *Arthritis Rheum*. 1988; 31(12):1500–1507. [PubMed: 3143369]
13. Carter DR, Beaupre GS, Giori NJ, Helms JA. Mechanobiology of skeletal regeneration. *Clin Orthop Relat Res*. 1998; (355 Suppl):S41–S55. [PubMed: 9917625]
14. Brighton CT, Hunt RM. Early histological and ultrastructural changes in medullary fracture callus. *J Bone Joint Surg Am*. 1991; 73(6):832–847. [PubMed: 2071617]
15. Tsunoda M, Mizuno K, Matsubara T. The osteogenic potential of fracture hematoma and its mechanism on bone formation—through fracture hematoma culture and transplantation of freeze-dried hematoma. *Kobe J Med Sci*. 1993; 39(1):35–50. [PubMed: 8366663]
16. Ho ML, Chang JK, Wang GJ. Antiinflammatory drug effects on bone repair and remodeling in rabbits. *Clin Orthop Relat Res*. 1995; (313):270–278. [PubMed: 7641490]
17. Simon AM, Manigrasso MB, O'Connor JP. Cyclo-oxygenase 2 function is essential for bone fracture healing. *J Bone Miner Res*. 2002; 17(6):963–976. [PubMed: 12054171]
18. Gebhard JS, Johnston-Jones K, Kody MH, Kabo JM, Meals RA. Effects of antihistamines on joint stiffness and bone healing after periarticular fracture. *J Hand Surg [Am]*. 1993; 18(6):1080–1085.
19. Hogevoid HE, Groggaard B, Reikeras O. Effects of short-term treatment with corticosteroids and indomethacin on bone healing. A mechanical study of osteotomies in rats. *Acta Orthop Scand*. 1992; 63(6):607–611. [PubMed: 1471505]
20. Andrew JG, Andrew SM, Freemont AJ, Marsh DR. Inflammatory cells in normal human fracture healing. *Acta Orthop Scand*. 1994; 65(4):462–466. [PubMed: 7976298]
21. Henricson A, Hulth A, Johnell O. The occurrence of accessory immunologic cells in bone induction. *Clin Orthop Relat Res*. 1991; (264):270–277. [PubMed: 1997246]
22. Askalonov AA, Gordienko SM, Avdyunicheva OE, Bondarenko AV, Voronkov SF. The role of T-system immunity in reparatory regeneration of the bone tissue in animals. *J Hyg Epidemiol Microbiol Immunol*. 1987; 31(2):219–224.
23. Askalonov AA. Changes in some indices of cellular immunity in patients with uncomplicated and complicated healing of bone fractures. *J Hyg Epidemiol Microbiol Immunol*. 1981; 25(3):307–310.
24. Santavirta S, Kontinen YT, Nordstrom D, Makela A, Sorsa T, Hukkanen M, et al. Immunologic studies of nonunited fractures. *Acta Orthop Scand*. 1992; 63(6):579–586. [PubMed: 1471500]
25. Hauser CJ, Zhou X, Joshi P, Cuchens MA, Kregor P, Devidas M, et al. The immune microenvironment of human fracture/soft-tissue hematomas and its relationship to systemic immunity. *J Trauma*. 1997; 42(5):895–903. discussion 903–904. [PubMed: 9191672]
26. Kon T, Cho TJ, Aizawa T, Yamazaki M, Nooh N, Graves D, et al. Expression of osteoprotegerin, receptor activator of NF-kappaB ligand (osteoprotegerin ligand) and related proinflammatory cytokines during fracture healing. *J Bone Miner Res*. 2001; 16(6):1004–1014. [PubMed: 11393777]
27. Kong YY, Yoshida H, Sarosi I, Tan HL, Timms E, Capparelli C, et al. OPGL is a key regulator of osteoclastogenesis, lymphocyte development and lymph-node organogenesis. *Nature*. 1999; 397(6717):315–323. [PubMed: 9950424]
28. Janeway CA Jr, Jones B, Hayday A. Specificity and function of T cells bearing gamma delta receptors. *Immunol Today*. 1988; 9(3):73–76. [PubMed: 2978457]

29. Lochner M, Peduto L, Cherrier M, Sawa S, Langa F, Varona R, et al. In vivo equilibrium of proinflammatory IL-17+ and regulatory IL-10+ Foxp3+ RORgamma t+ T cells. *J Exp Med*. 2008; 205(6):1381–1393. [PubMed: 18504307]
30. Beetz S, Wesch D, Marischen L, Welte S, Oberg HH, Kabelitz D. Innate immune functions of human gammadelta T cells. *Immunobiology*. 2008; 213(3–4):173–182. [PubMed: 18406365]
31. Ferrick DA, Schrenzel MD, Mulvania T, Hsieh B, Ferlin WG, Lepper H. Differential production of interferon-gamma and interleukin-4 in response to Th1- and Th2-stimulating pathogens by gamma delta T cells in vivo. *Nature*. 1995; 373(6511):255–257. [PubMed: 7816142]
32. Holoshitz J, Koning F, Coligan JE, De Bruyn J, Strober S. Isolation of CD4- CD8- mycobacteria-reactive T lymphocyte clones from rheumatoid arthritis synovial fluid. *Nature*. 1989; 339(6221):226–229. [PubMed: 2524009]
33. Moore TA, Moore BB, Newstead MW, Standiford TJ. Gamma delta-T cells are critical for survival and early proinflammatory cytokine gene expression during murine *Klebsiella pneumoniae*. *J Immunol*. 2000; 165(5):2643–2650. [PubMed: 10946293]
34. Daniel T, Thobe BM, Chaudry IH, Choudhry MA, Hubbard WJ, Schwacha MG. Regulation of the postburn wound inflammatory response by gammadelta T-cells. *Shock*. 2007; 28(3):278–283. [PubMed: 17545947]
35. Corthay A, Johansson A, Vestberg M, Holmdahl R. Collagen-induced arthritis development requires alpha beta T cells but not gamma delta T cells: studies with T cell-deficient (TCR mutant) mice. *Int Immunol*. 1999; 11(7):1065–1073. [PubMed: 10383939]
36. O'Brien RL, Born W. Heat shock proteins as antigens for gamma delta T cells. *Semin Immunol*. 1991; 3(2):81–87. [PubMed: 1832320]
37. Havran WL, Chien YH, Allison JP. Recognition of self antigens by skin-derived T cells with invariant gamma delta antigen receptors. *Science*. 1991; 252(5011):1430–1432. [PubMed: 1828619]
38. Jameson J, Ugarte K, Chen N, Yachi P, Fuchs E, Boismenu R, et al. A role for skin gammadelta T cells in wound repair. *Science*. 2002; 296(5568):747–749. [PubMed: 11976459]
39. Kelleher D, Murphy A, Feighery C, Casey EB. Leukocyte function-associated antigen 1 (LFA-1) and CD44 are signalling molecules for cytoskeleton-dependent morphological changes in activated T cells. *J Leukoc Biol*. 1995; 58(5):539–546. [PubMed: 7595055]
40. Yamazaki M, Nakajima F, Ogasawara A, Moriya H, Majeska RJ, Einhorn TA. Spatial and temporal distribution of CD44 and osteopontin in fracture callus. *J Bone Joint Surg Br*. 1999; 81(3):508–515. [PubMed: 10872376]
41. Jameson JM, Cauvi G, Sharp LL, Witherden DA, Havran WL. Gammadelta T cell-induced hyaluronan production by epithelial cells regulates inflammation. *J Exp Med*. 2005; 201(8):1269–1279. [PubMed: 15837812]
42. Itohara S, Mombaerts P, Lafaille J, Iacomini J, Nelson A, Clarke AR, et al. T cell receptor delta gene mutant mice: independent generation of alpha beta T cells and programmed rearrangements of gamma delta TCR genes. *Cell*. 1993; 72(3):337–348. [PubMed: 8381716]
43. Bos GD, Goldberg VM, Powell AE, Heiple KG, Zika JM. The effect of histocompatibility matching on canine frozen bone allografts. *J Bone Joint Surg Am*. 1983; 65(1):89–96. [PubMed: 6336761]
44. Hsu SM, Raine L, Fanger H. Use of avidin-biotin-peroxidase complex (ABC) in immunoperoxidase techniques: a comparison between ABC and unlabeled antibody (PAP) procedures. *J Histochem Cytochem*. 1981; 29(4):577–580. [PubMed: 6166661]
45. Fujii H, Kitazawa R, Maeda S, Mizuno K, Kitazawa S. Expression of platelet-derived growth factor proteins and their receptor alpha and beta mRNAs during fracture healing in the normal mouse. *Histochem Cell Biol*. 1999; 112(2):131–138. [PubMed: 10460466]
46. Metsaranta M, Toman D, de Crombrugge B, Vuorio E. Mouse type II collagen gene. Complete nucleotide sequence, exon structure, and alternative splicing. *J Biol Chem*. 1991; 266(25):16862–16869. [PubMed: 1885613]
47. Young MF, Ibaraki K, Kerr JM, Lyu MS, Kozak CA. Murine bone sialoprotein (BSP): cDNA cloning, mRNA expression, and genetic mapping. *Mamm Genome*. 1994; 5(2):108–111. [PubMed: 8180469]

48. Feng JQ, Harris MA, Ghosh-Choudhury N, Feng M, Mundy GR, Harris SE. Structure and sequence of mouse bone morphogenetic protein-2 gene (BMP-2): comparison of the structures and promoter regions of BMP-2 and BMP-4 genes. *Biochim Biophys Acta*. 1994; 1218(2):221–224. [PubMed: 8018727]
49. Eshbach, OW.; Sounders, M. *Handbook of Engineering Fundamentals*. 3 ed. New York: Wiley; 1975.
50. Dumbleton, JH.; Black, J. *Clinical Biomechanics*. Black, J.; Dumbleton, JH., editors. New York: Churchill Livingstone; 1981. p. 359-400.
51. Matsushima A, Ogura H, Fujita K, Koh T, Tanaka H, Sumi Y, et al. Early activation of gammadelta T lymphocytes in patients with severe systemic inflammatory response syndrome. *Shock*. 2004; 22(1):11–15. [PubMed: 15201695]
52. Jingushi S, Joyce ME, Bolander ME. Genetic expression of extracellular matrix proteins correlates with histologic changes during fracture repair. *J Bone Miner Res*. 1992; 7(9):1045–1055. [PubMed: 1414497]
53. Hamzaoui K, Hamzaoui A, Hentati F, Kahan A, Ayed K, Chabbou A, et al. Phenotype and functional profile of T cells expressing gamma delta receptor from patients with active Behcet's disease. *J Rheumatol*. 1994; 21(12):2301–2306. [PubMed: 7699633]
54. Aguilar MM, Battistella FD, Owings JT, Olson SA, MacColl K. Posttraumatic lymphocyte response: a comparison between peripheral blood T cells and tissue T cells. *J Trauma*. 1998; 45(1): 14–18. [PubMed: 9680005]
55. Roark CL, French JD, Taylor MA, Bendele AM, Born WK, O'Brien RL. Exacerbation of collagen-induced arthritis by oligoclonal, IL-17-producing gamma delta T cells. *J Immunol*. 2007; 179(8): 5576–5583. [PubMed: 17911645]

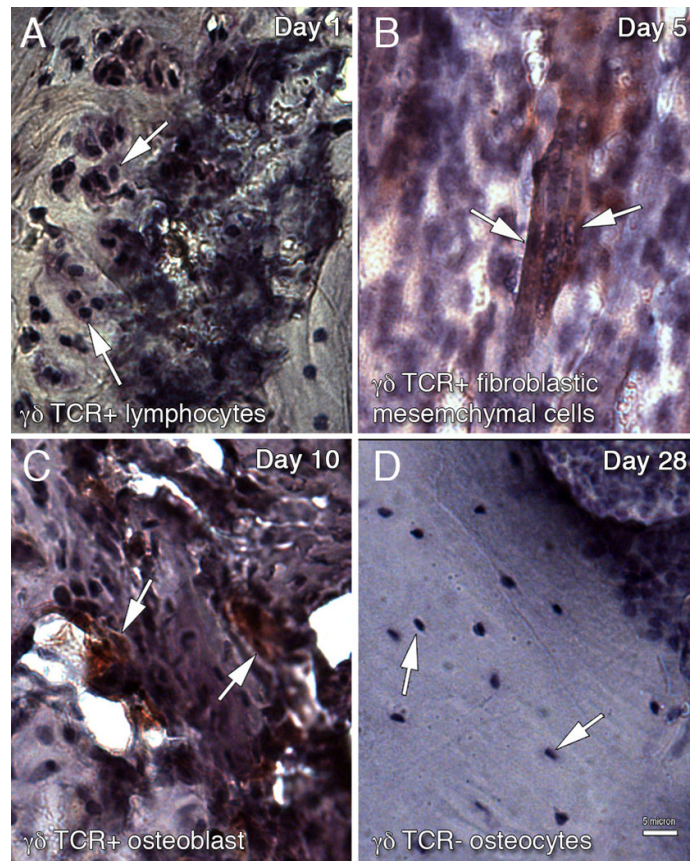


Figure 1. Immunohistochemical localization of $\gamma\delta$ T-cell in the tibia fracture site of control wild-type mice. $\gamma\delta$ T-cells were detected using monoclonal antibodies to $\gamma\delta$ TCR followed by HRP-conjugated secondary antibodies. Peroxidase-positive is shown as red colored deposit. Arrows point to TCR+ cells in A–C and TCR– cells in D. Four phases of fracture repair were examined: (A) Day 1, hematoma with $\gamma\delta$ TCR+ lymphocytes (B) Day 5, $\gamma\delta$ TCR+ mesenchymal cells (C) Day 10, $\gamma\delta$ TCR+ osteoblast and (D) Day 28, $\gamma\delta$ TCR– osteocytes. Scale bar = 5 μ m

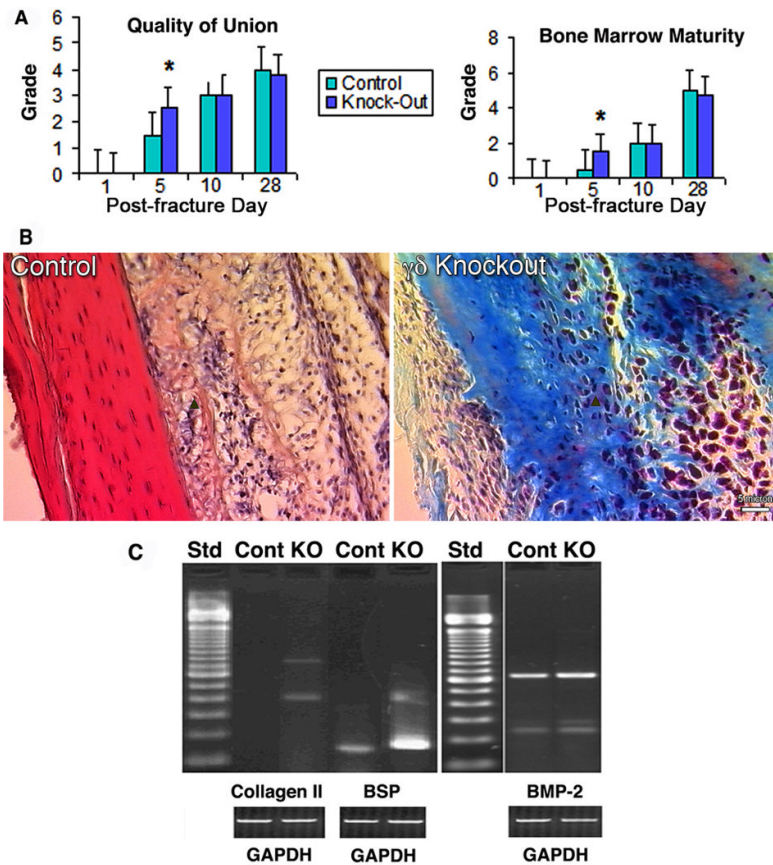


Figure 2.

Histological and gene expression analyses of fracture repair in control and $\gamma\delta$ knockout mice. (A) Comparative histology scores based on quality of union (left) and colonization of marrow (right). Scores are expressed as mean \pm standard deviation. Day 5 knockout animals had higher scores in both categories. *, $p < 0.05$. (B) Representative histology for the reparative phase at Day 5. Arrows point to new osseous elements formed in each group, which are more apparent in knockout animals as compared to controls. Scale bar = 5 μ m. (C) Gene expression profile of collagen type II, BSP, and BMP-2 in control and $\gamma\delta$ knockout mice on Day 5 post-fracture. $\gamma\delta$ knockout animal showed increased expression of all three genes compared with controls.

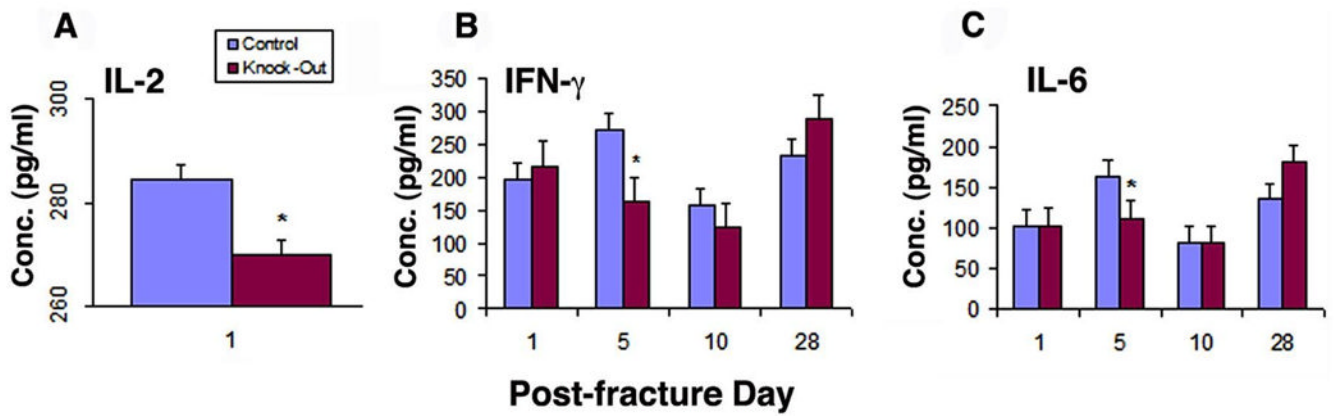


Figure 3.

Cytokine response post-fracture in the fracture site of control and $\gamma\delta$ knockout animals analyzed by ELISA. (A) IL-2. An overall decrease in IL-2 is seen in $\gamma\delta$ knockout animal during the inflammatory phase (Day 1) as compared with controls. (B) Interferon- γ and (C) IL-6. These proinflammatory cytokines are reduced at the reparative phase (Day 5) in $\gamma\delta$ knockout animals as compared to controls. All values are expressed as mean \pm standard deviation *, $p < 0.05$.

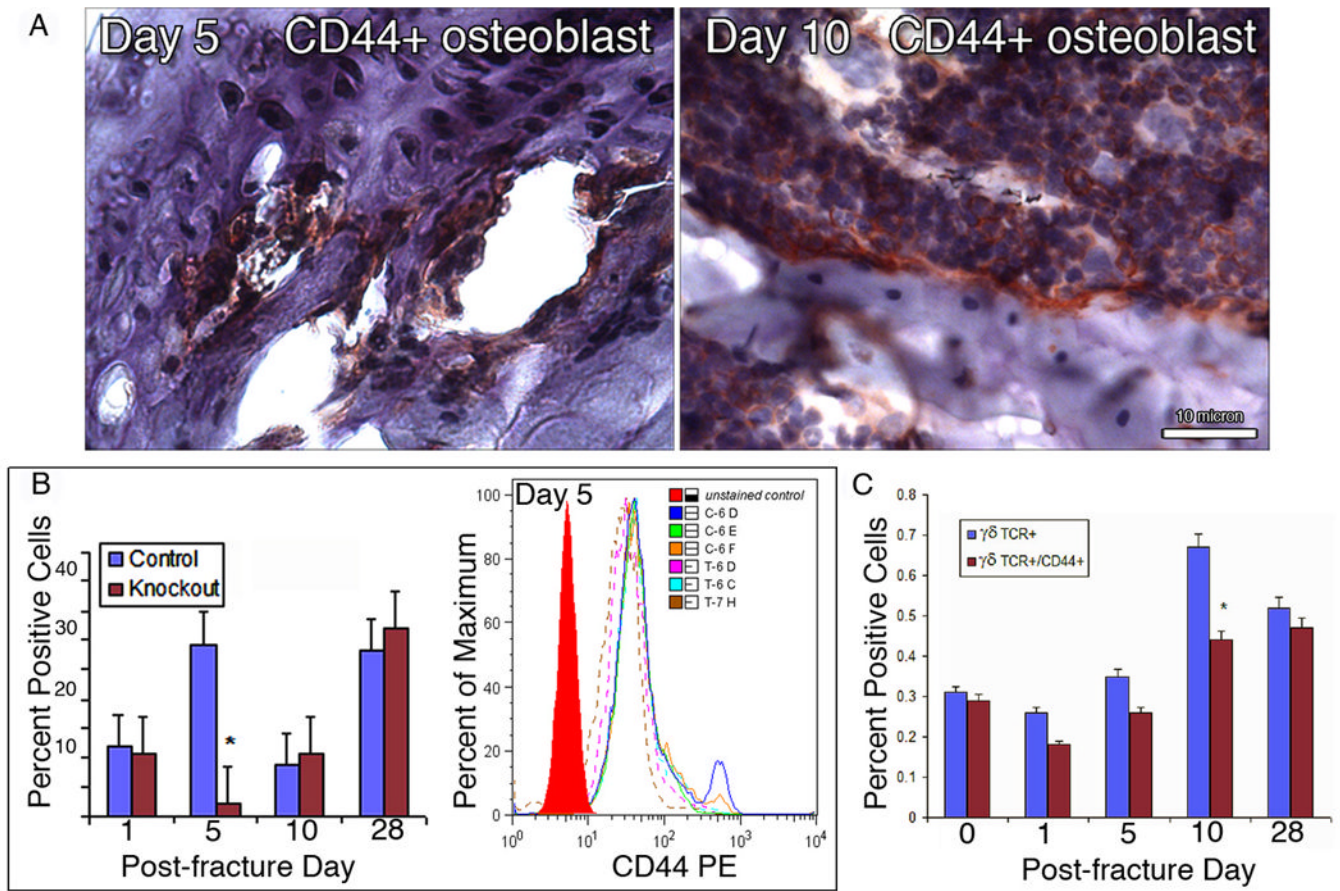


Figure 4.

Receptor expression post fracture. (A) Immunohistochemistry. $\gamma\delta$ knockout animals showed presence of CD44 cell adhesion molecule (red colored deposit) on osteoblasts (arrow) during the reparative phases (Day 5, left, and Day 10, right). Scale bar = 10 μ m. (B) Flow cytometry Percentage of total peripheral lymphocytes expressing the CD44 surface marker. A significant decrease in CD44 + lymphocytes is seen in $\gamma\delta$ knockout animals on Day 5. (C) Presence of $\gamma\delta$ TCR+ and $\gamma\delta$ TCR+/CD44+ lymphocytes at the systemic level in control wild type animals.

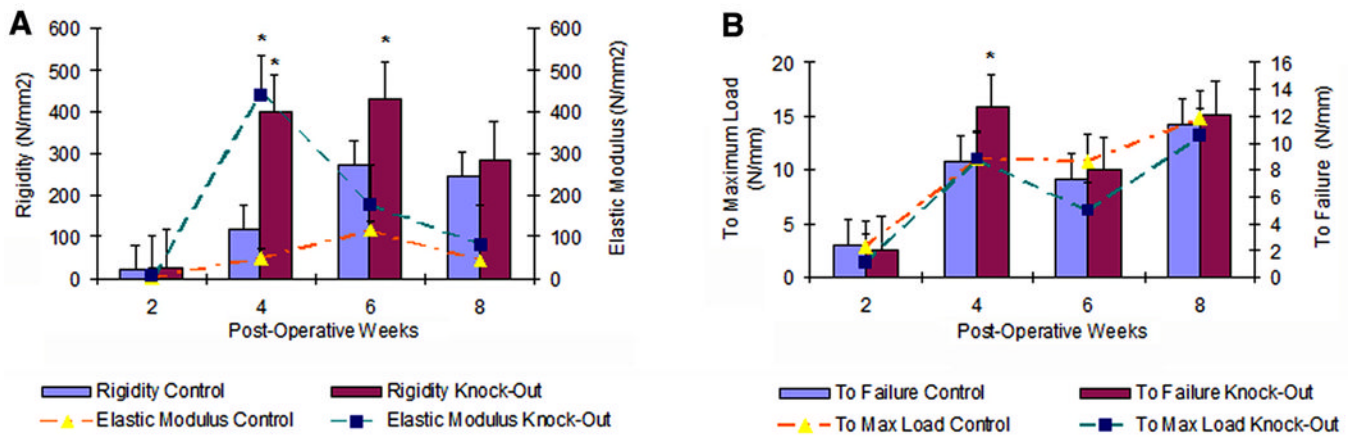


Figure 5. Mechanical testing analysis of fracture repair in control and $\gamma\delta$ knockout animals. (A) Material and structural strengths of the healing callus. (B) Energy absorption by the healing callus to maximum load and failure. All values are expressed as mean \pm standard deviation. *, $p < 0.05$

Table 1

Receptor Expression in $\gamma\delta$ Knockout and Control Mice

Cell or tissue		$\gamma\delta$ T						CD44					
		Days post fracture			Days post fracture			Days post fracture			Days post fracture		
		1	5	28	1	5	28	1	5	10	28		
Hematoma	Control	+	-	-	-	-	-	-	-	-	-	-	-
	KO	-	-	-	-	-	-	-	±	-	-	-	-
Inflammatory cells	Control	+	-	-	-	-	+	-	-	-	-	-	-
	KO	-	-	-	-	-	-	±	-	-	-	-	-
Mesenchymal cells	Control	+	+	++	-	-	+	+	+	+	-	-	-
	KO	-	-	-	-	-	±	±	±	±	-	-	-
Connective tissue	Control	+	+	+	-	-	+	+	+	+	+	+	+
	KO	-	-	-	-	-	+	+	±	+	+	+	-
Chondrocytes	Control	-	-	±	-	-	-	-	-	-	-	-	-
	KO	-	-	-	-	-	-	-	-	-	-	-	-
Osteoblasts	Control	-	-	+++	-	-	-	-	-	+	-	-	-
	KO	-	-	-	-	-	-	-	-	±	+	-	-
Osteoclasts	Control	-	-	++	-	-	-	-	-	+	+	+	+
	KO	-	-	-	-	-	-	-	-	+	+	-	-
Osteocytes	Control	-	-	-	-	-	-	-	-	-	-	±	±
	KO	-	-	-	-	-	-	-	-	±	-	-	+